

---

# **Stepwise chemical oxidation to accessing ultrathin metal (oxy)-hydroxide nanosheets for oxygen evolution reaction**

Jiangquan Lv,<sup>\*a,b</sup> Xiangfeng Guan,<sup>a,b</sup> Yiyin Huang,<sup>\*c</sup> Lanxin Cai,<sup>a</sup> Muxin Yu,<sup>a</sup> Xiaoyan Li,<sup>a</sup> Yunlong Yu,<sup>a</sup> and Dagui Chen<sup>a</sup>

## **Table of Contents**

- 1. Supplementary Figures.**
- 2. Supplementary Tables.**
- 3. Supplementary References.**

## 1. Supplementary Figures.

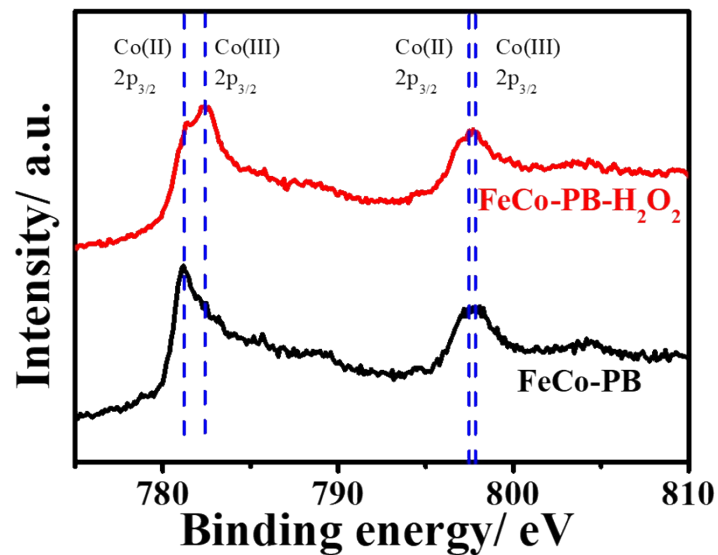


**Figure S1.** High-resolution Co 2p spectra of the FeCo-PB and FeCo-PB-H<sub>2</sub>O<sub>2</sub>.

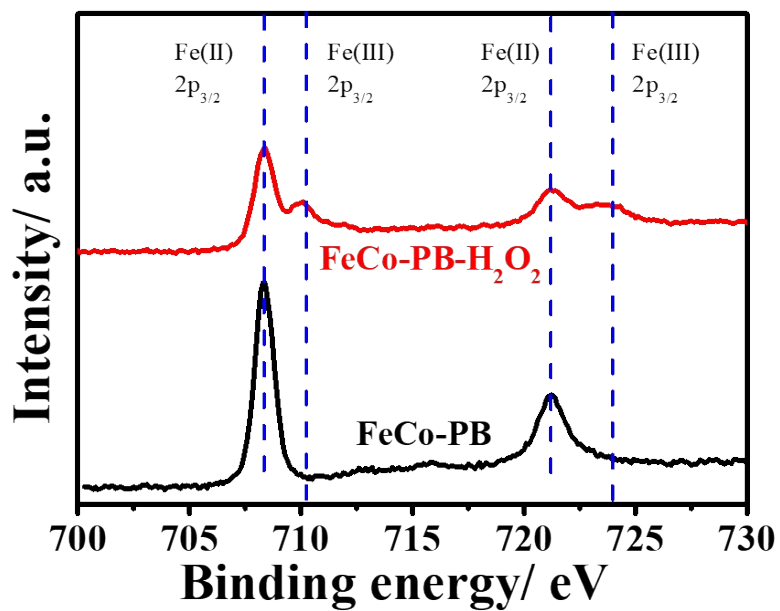


**Figure S2.** High-resolution Fe 2p spectra of the FeCo-PB and FeCo-PB-H<sub>2</sub>O<sub>2</sub>.

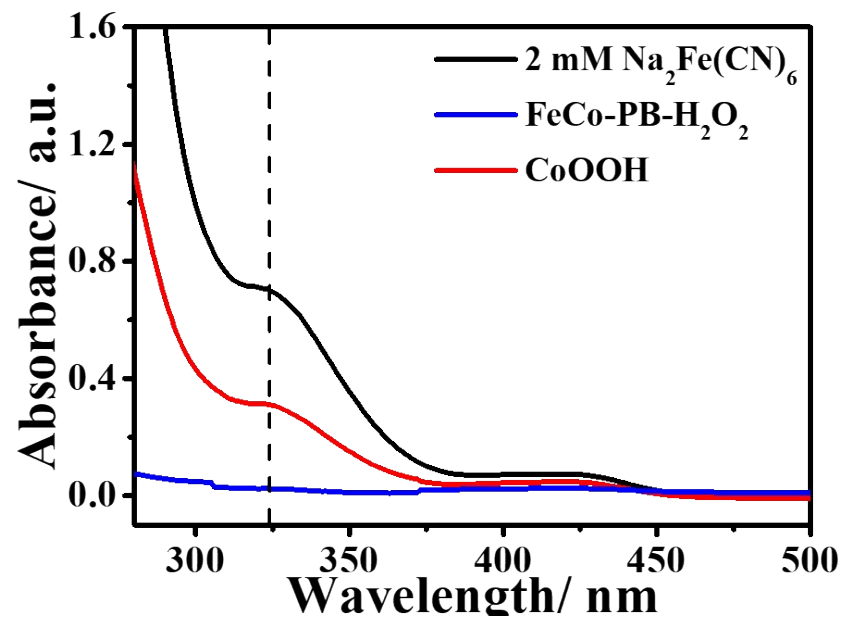


**Figure S3.** UV-vis absorption spectra of 2 mM  $\text{Na}_2\text{Fe}(\text{CN})_6$  and the solution after  $\text{H}_2\text{O}_2$  oxidation (FeCo-PB- $\text{H}_2\text{O}_2$ ) and two-step oxidation (CoOOH).

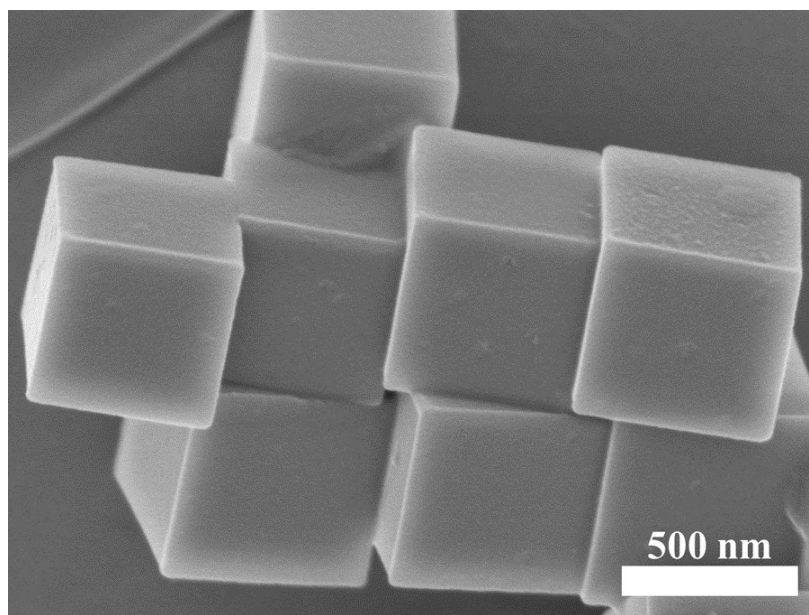


**Figure S4.** SEM image of FeCo-PB showed a cubic morphology with dimensions of about 550 nm.

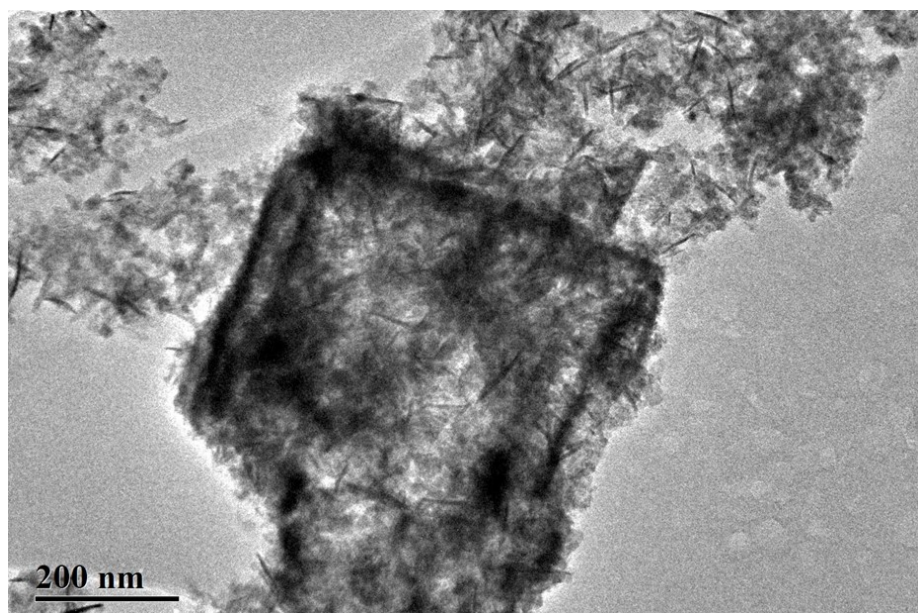


**Figure S5.** The TEM image of FeCo-PB-NaClO showed a deficient structure transformation.

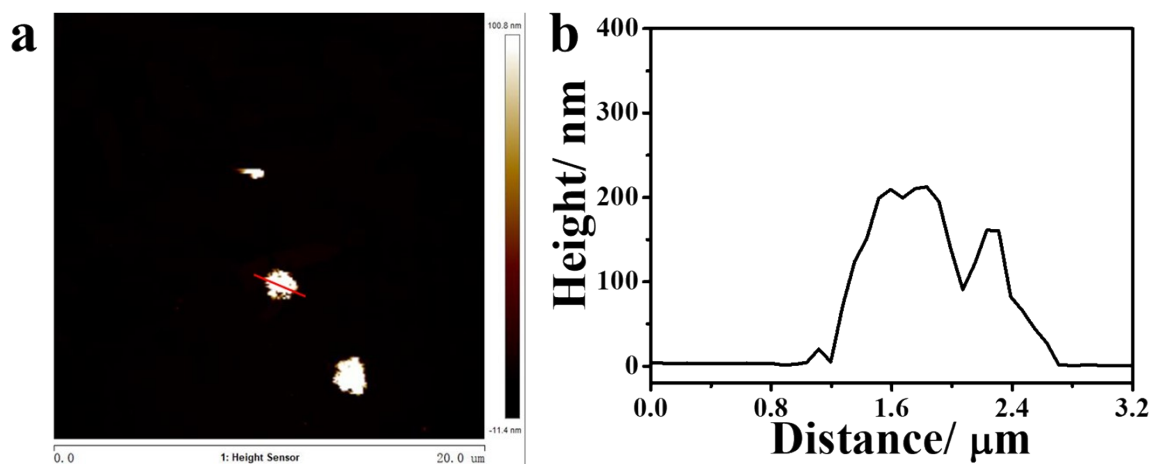


**Figure S6.** (a) Representative AFM image of FeCo-PB-NaClO and (b) the corresponding thickness analysis taken around the red line in (a).

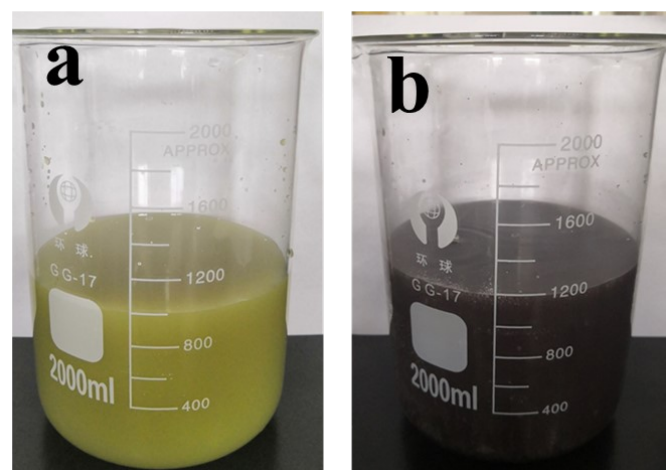


**Figure S7.** Digital images of (a) FeCo-PB and (b) FeCo-PB-H<sub>2</sub>O<sub>2</sub>.

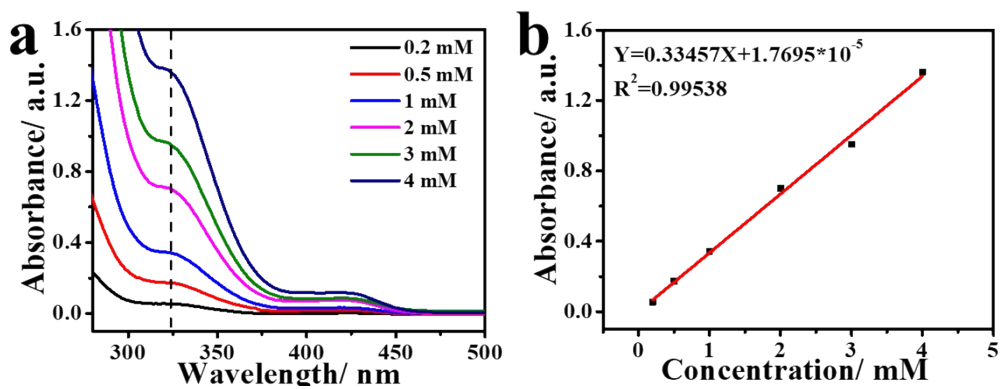


**Figure S8.** (a) UV-vis absorption spectra of different concentrations of  $\text{Na}_2\text{Fe}(\text{CN})_6$  (range from 0.2 mM to 4 mM); (b) Calibration curve used for calculation of  $\text{Fe}(\text{CN})_6^{2-}$  concentrations.

The absorbance of the solution after two-step oxidation was 0.31, according to the equation, the concentration was calculated to be 0.9265 mmol/L. The theoretical  $\text{Fe}(\text{CN})_6^{2-}$  concentration of 500 mg  $\text{Na}_2\text{Fe}(\text{CN})_6$  in final 1600 mL solution was 0.9864 mmol/L, so the recycling ratio of  $\text{Fe}(\text{CN})_6^{2-}$  was calculated to be 93.8%.

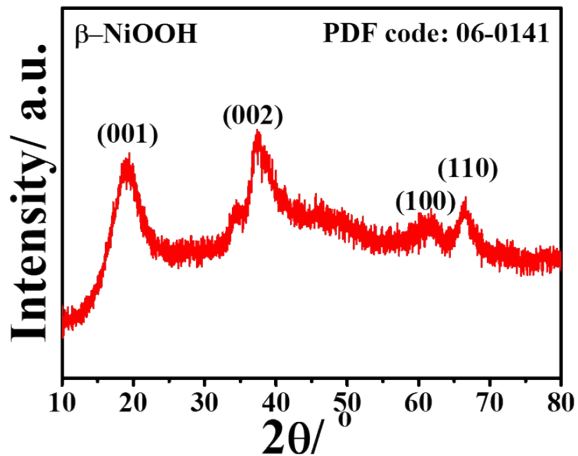


**Figure S9.** XRD pattern of  $\beta$ -NiOOH, which synthesized by two-step oxidation procedure of  $\text{Na}_x\text{NiFe}(\text{CN})_6$ .

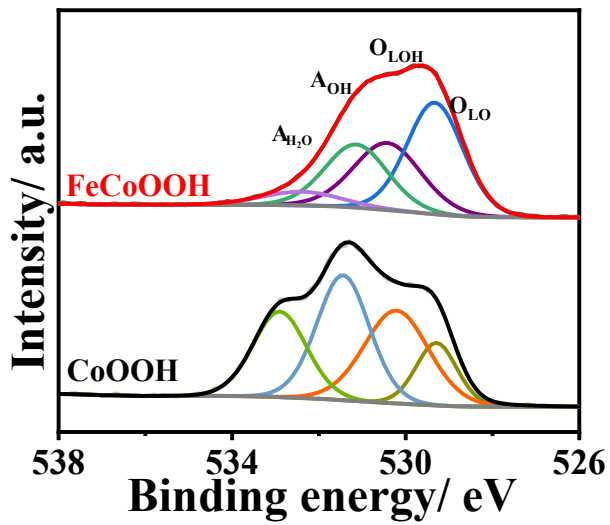


**Figure S10.** High-resolution O 1s spectra of the FeCoOOH nanosheets and CoOOH nanosheets;

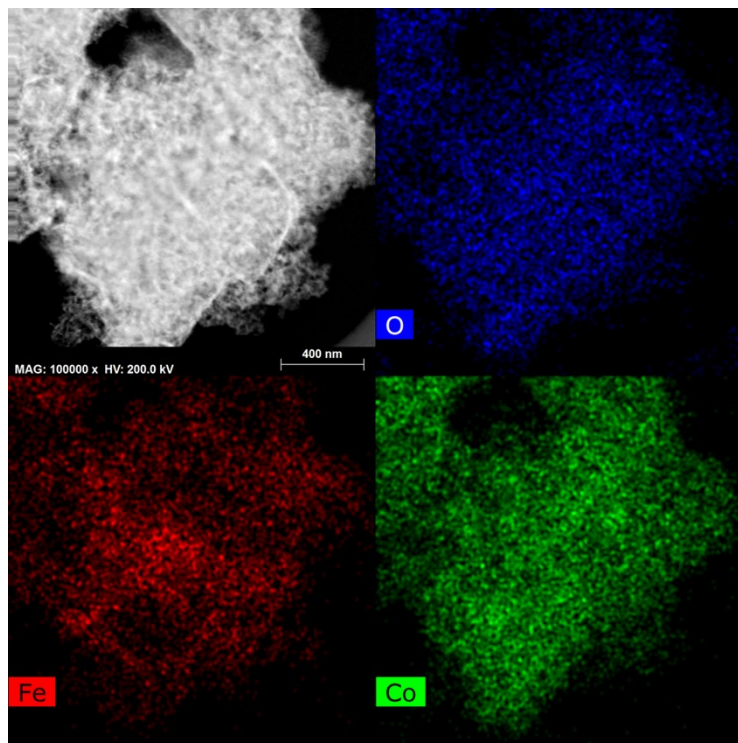


**Figure S11.** Element mapping of FeCoOOH nanosheets with O, Fe and Co.

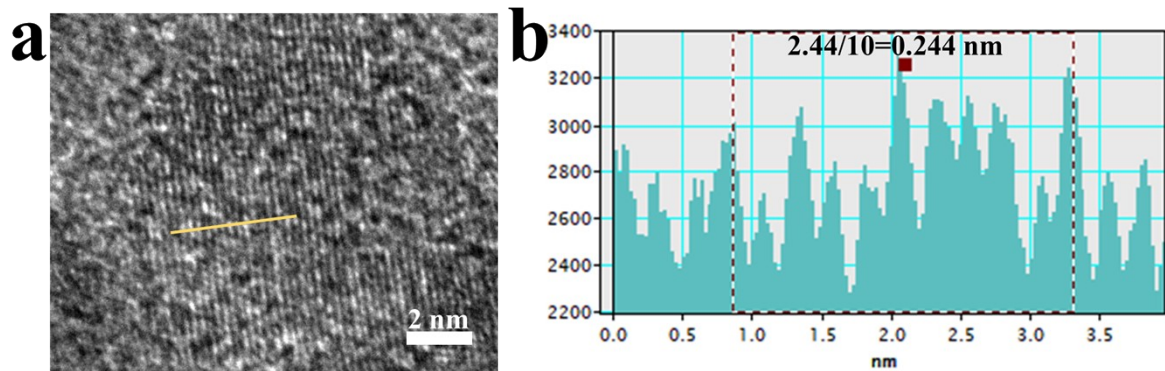


**Figure S12.** (a) HRTEM image of FeCoOOH nanosheets; (b) the profile of HRTEM for the calculation of lattice fringes.

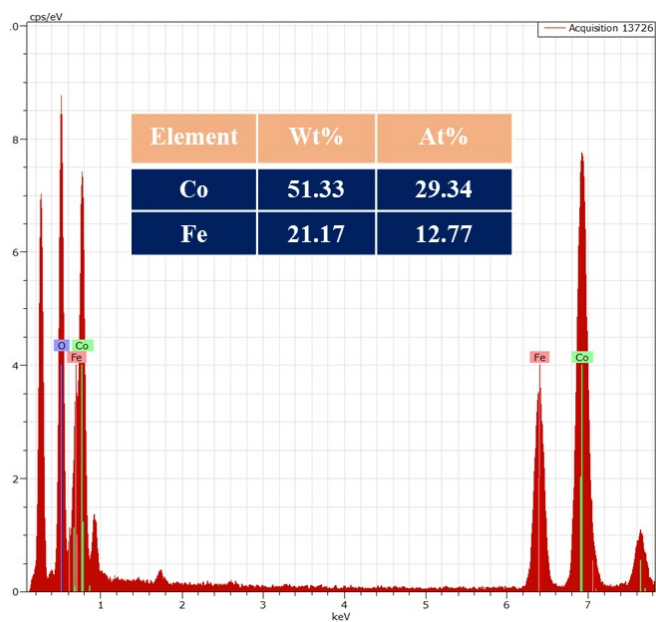


**Figure S13.** EDS result of FeCoOOH.

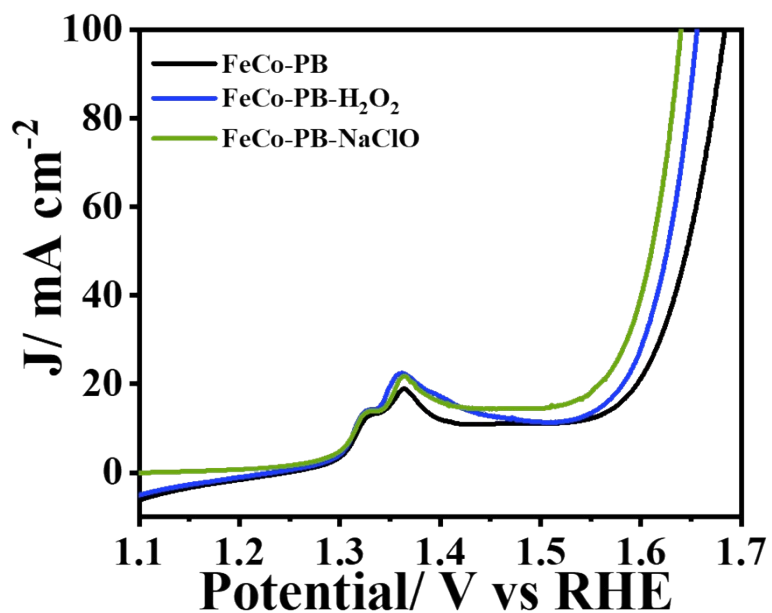


**Figure S14.** LSV plots of FeCo-PB, FeCo-PB- $\text{H}_2\text{O}_2$  and FeCo-PB- $\text{NaClO}$ .

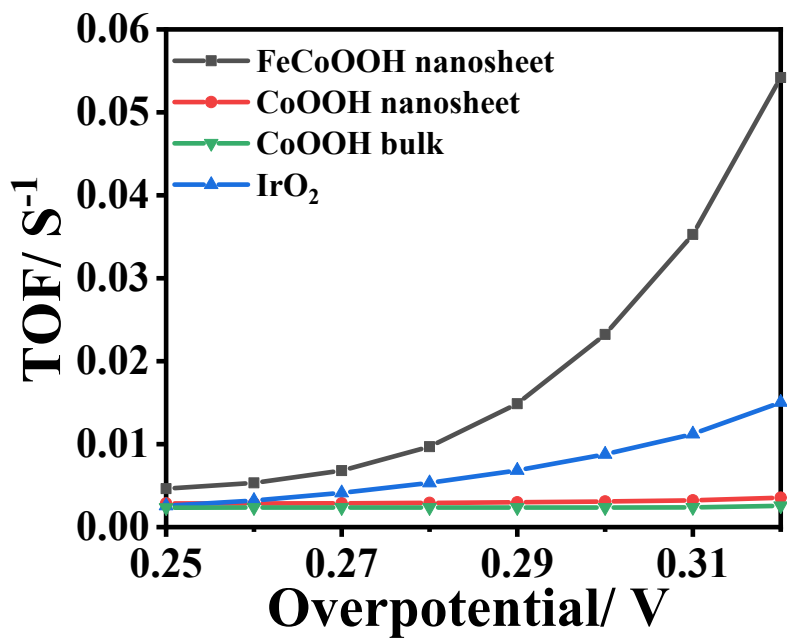


**Figure S15.** TOF plots of FeCoOOH nanosheet, CoOOH nanosheet, CoOOH bulk and IrO<sub>2</sub> at different overpotentials.

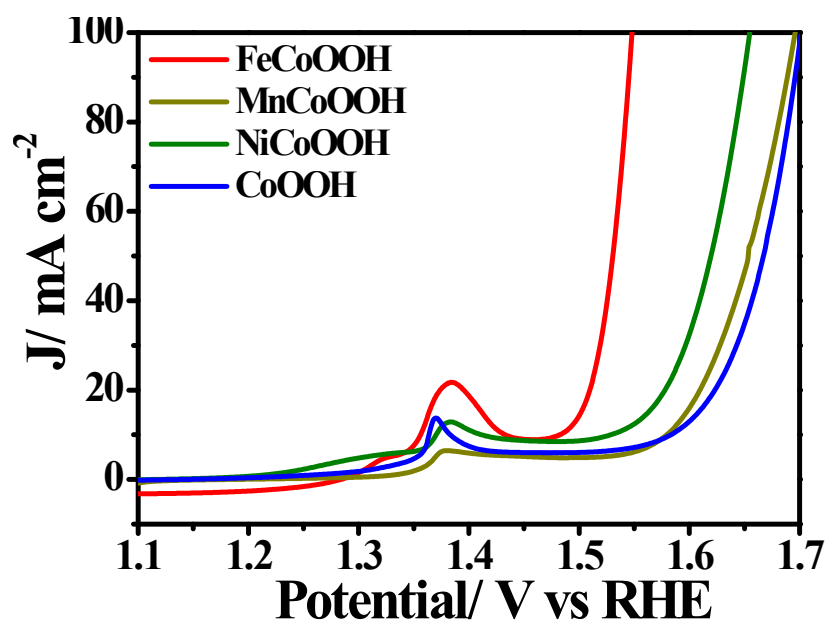


**Figure S16.** LSV plots of FeCoOOH, MnCoOOH, NiCoOOH and CoOOH.

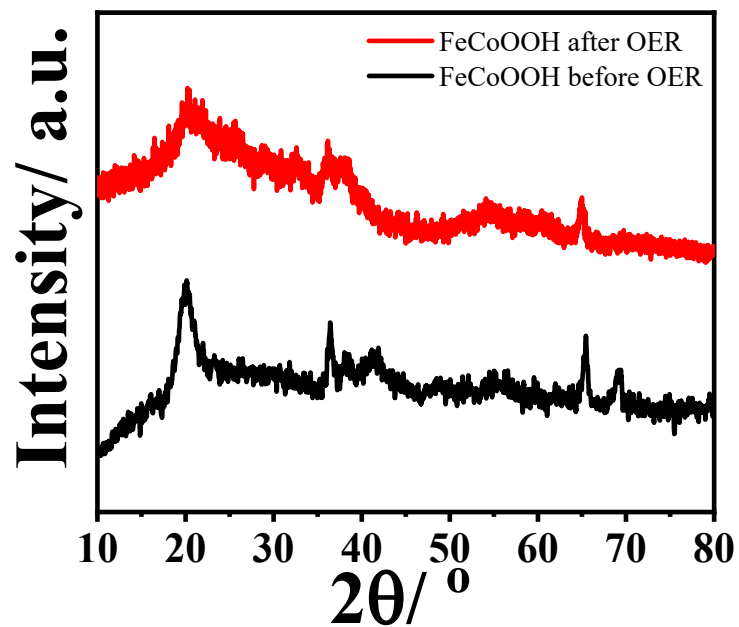


**Figure S17.** XRD patterns of FeCoOOH nanosheets before and after OER stability test.

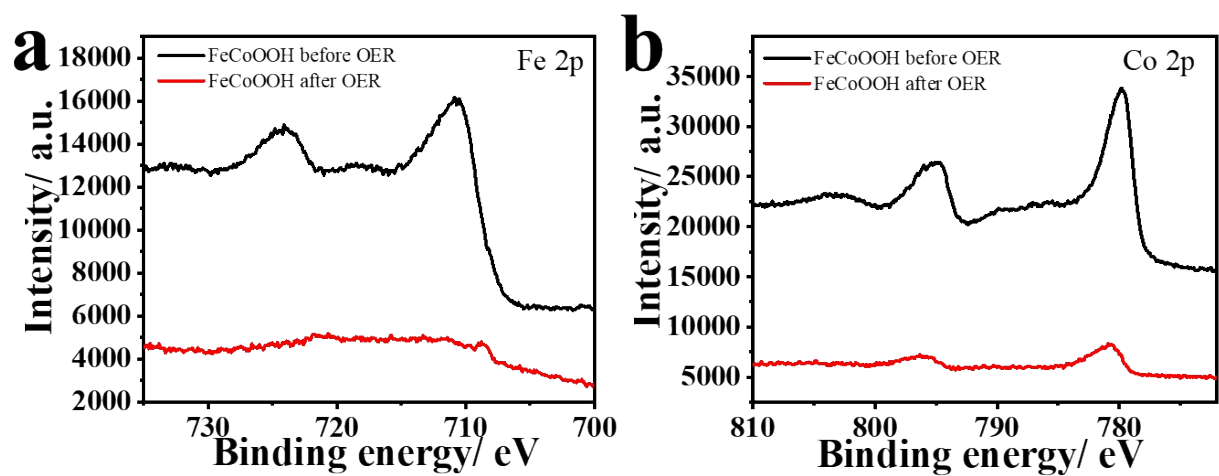


**Figure S18.** (a) Co 2p XPS spectra and (b) Fe 2p XPS spectra for FeCoOOH nanosheets before and after OER stability test.

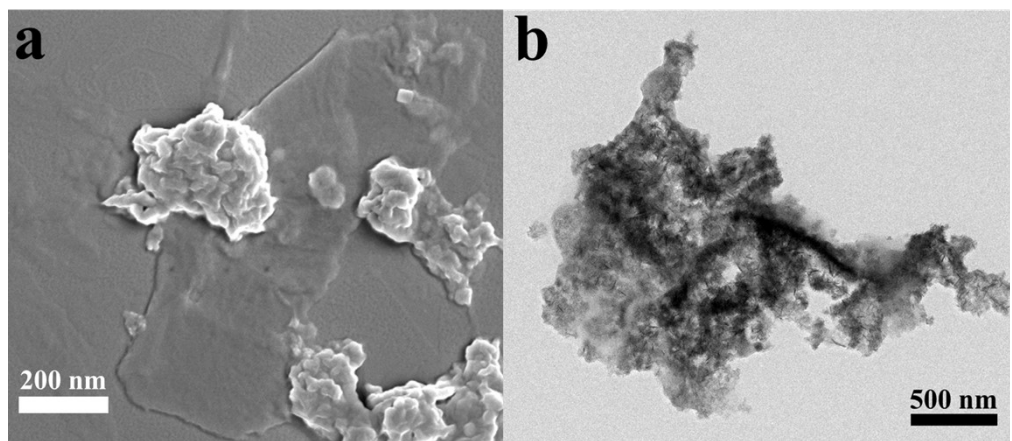


**Figure S19.** (a) SEM and (b) TEM images for FeCoOOH nanosheets after OER stability test.

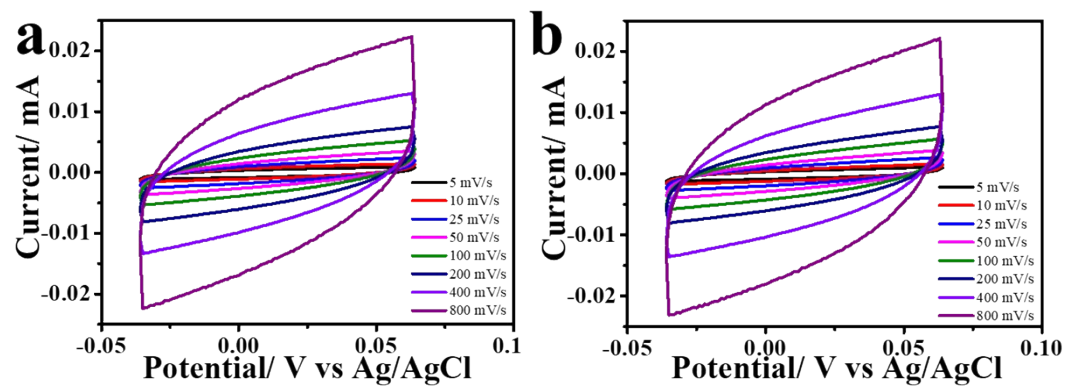


**Figure S20.** CV curves of (a) CoOOH and (b) FeCoOOH at scan rates ranging from  $5 \text{ mV s}^{-1}$  to  $800 \text{ mV s}^{-1}$ .

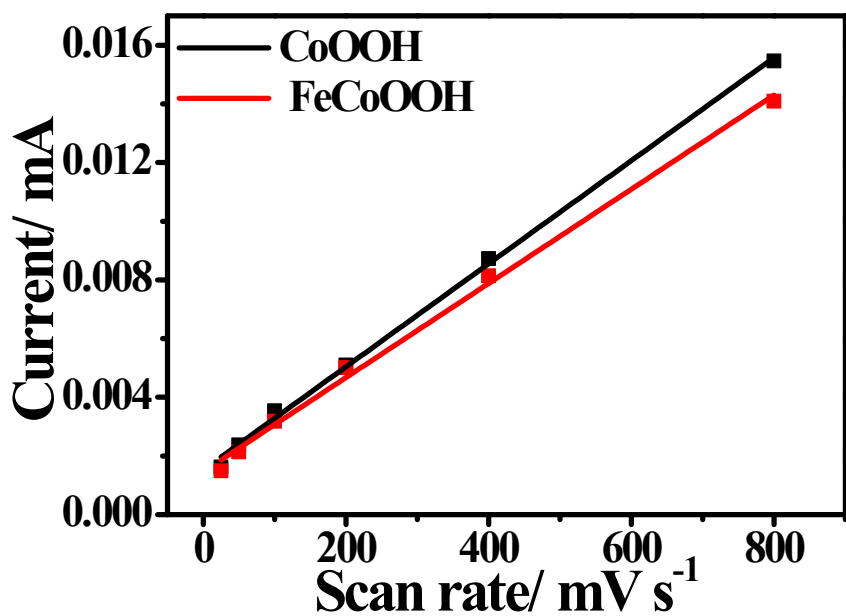


**Figure S21.** Calculation of  $C_{dl}$  for CoOOH and FeCoOOH by plotting the capacitive current density against the scan rate to fit a linear regression.

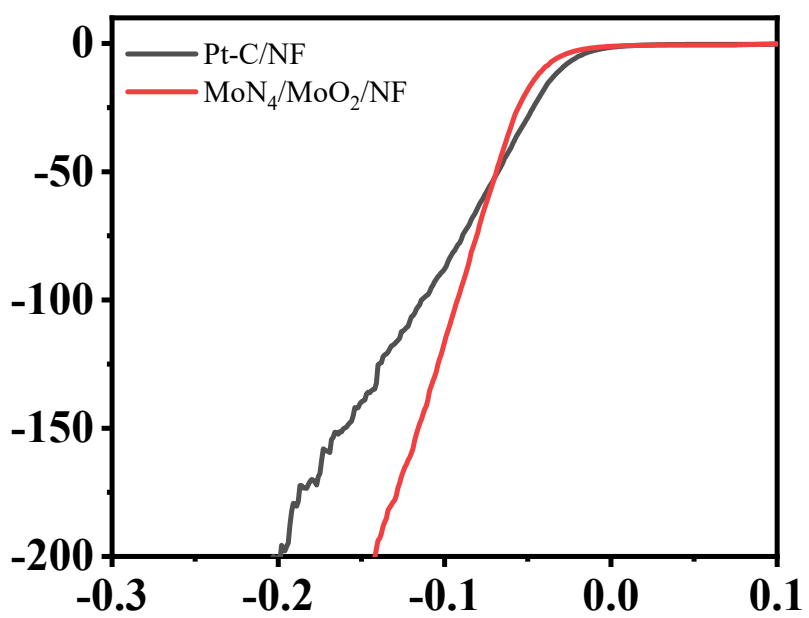


**Figure S22.** LSV polarization curve of  $\text{MoNi}_4/\text{MoO}_2/\text{NF}$  and Pt-C/NF for HER with 90% iR-compensation.

## 2. Supplementary Table.

**Table S1.** Comparison of OER activities of different cobalt-based materials.

Catalyst	Electrolyt e	Overpotential at 10 mA cm <sup>-2</sup> (mV)	Substrate	Reference
FeCoOOH	1 M KOH	252	Ni foam	This work
Fe/CoOOH	1 M KOH	266	Carbon cloth	S1
Co-PBA-plasma 2 h	1 M KOH	274	Ni foam	S2
FeCo-MOF-EH	1 M KOH	231	Ni foam	S3
$\gamma$ -CoOOH nanosheets	1 M KOH	275	Ni foam	S4
Co <sub>2</sub> AlO <sub>4</sub> nanosheets	1 M KOH	280	Carbon paper	S5
Co <sub>3</sub> O <sub>4</sub> -CoO nanosheets	1 M KOH	270	Carbon cloth	S6
nPBA@Co(OH) <sub>2</sub> /NF	1 M KOH	258	Ni foam	S7
F-CoOOH/NF	1 M KOH	270	Ni foam	S8
Co(OH) <sub>2</sub> /NCNTs-NF	1 M KOH	270	Ni foam	S9
CoCO <sub>3</sub> @CoSe Nanowires	1 M KOH	255	Ni foam	S10
CoS	1 M KOH	297	Ni foam	S11

**Table S2.** Comparison of overall water splitting performance in recent reports.

Catalyst	Electrolyte	Potential at 10 mA cm <sup>-2</sup> (V)	Substrate	Reference
FeCoOOH	1 M KOH	1.50	Ni foam	This work
NiO–Ni <sub>3</sub> S <sub>2</sub> /NF	1 M KOH	1.57	Ni foam	S12
2D/3D ZIF-67@CC	1 M KOH	1.545	Carbon cloth	S13
Co <sub>3</sub> S <sub>4</sub> /EC-MOF	1 M KOH	1.55	carbon cloth	S14
NC/CuCo/CuCoO <sub>x</sub>	1 M KOH	1.53	Ni foam	S15
1T-MoS <sub>2</sub>	1 M KOH	1.57	Glassy carbon	S16
Am FePO <sub>4</sub> /NF	1 M KOH	1.54	Ni foam	S17

## Supplementary References

- S1. S.-H. Ye, Z.-X. Shi, J.-X. Feng, Y.-X. Tong and G.-R. Li, *Angewandte Chemie-International Edition*, 2018, **57**, 2672-2676.
- S2. Y. Guo, T. Wang, J. Chen, J. Zheng, X. Li and K. Ostrikov, *Adv. Energy Mater.*, 2018, **8**, 1800085.
- S3. J. Tian, F. Jiang, D. Yuan, L. Zhang, Q. Chen and M. Hong, *Angewandte Chemie-International Edition*, 2020, **59**, 13101-13108.
- S4. H. Wang, E.-m. Feng, Y.-m. Liu and C.-y. Zhang, *J. Mater. Chem. A*, 2019, **7**, 7777-7783.
- S5. J. Wang, Y. Shen, G. Wei, W. Xi, X. Ma, W. Zhang, P. Zhu and C. An, *Science China Materials*, 2020, **63**, 91-99.
- S6. J. Qi, Y. Yan, T. Liu, X. Zhou, J. Cao and J. Feng, *Journal of Colloid and Interface Science*, 2020, **565**, 400-404.
- S7. Y. Wang, J. Ma, J. Wang, S. Chen, H. Wang and J. Zhang, *Adv. Energy Mater.*, 2019, **9**, 1802939.
- S8. P. Chen, T. Zhou, S. Wang, N. Zhang, Y. Tong, H. Ju, W. Chu, C. Wu and Y. Xie, *Angewandte Chemie-International Edition*, 2018, **57**, 15471-15475.
- S9. P. Guo, J. Wu, X.-B. Li, J. Luo, W.-M. Lau, H. Liu, X.-L. Sun and L.-M. Liu, *Nano Energy*, 2018, **47**, 96-104.
- S10. R. Que, G. Ji, D. Liu, M. Li, X. Wang and S. P. Jiang, *Energy Technology*, 2019, **7**, 1800741.
- S11. P. Guo, Y.-X. Wu, W.-M. Lau, H. Liu and L.-M. Liu, *Journal of Alloys and Compounds*, 2017, **723**, 772-778.
- S12. L. Peng, J. Shen, X. Zheng, R. Xiang, M. Deng, Z. Mao, Z. Feng, L. Zhang, L. Li and Z. Wei, *Journal Of Catalysis*, 2019, **369**, 345-351.
- S13. Z. Chen, Y. Ha, H. Jia, X. Yan, M. Chen, M. Liu and R. Wu, *Adv. Energy Mater.*, 2019, **9**, 1803918.
- S14. T. Liu, P. Li, N. Yao, T. Kong, G. Cheng, S. Chen and W. Luo, *Adv. Mater.*, 2019, **31**, 1806672.
- S15. J. Hou, Y. Sun, Y. Wu, S. Cao and L. Sun, *Adv. Funct. Mater.*, 2018, **28**, 1704447.
- S16. S. Wei, X. Cui, Y. Xu, B. Shang, Q. Zhang, L. Gu, X. Fan, L. Zheng, C. Hou, H. Huang, S. Wen and W. Zheng, *Acs Energy Letters*, 2019, **4**, 368-374.
- S17. L. Yang, Z. Guo, J. Huang, Y. Xi, R. Gao, G. Su, W. Wang, L. Cao and B. Dong, *Adv. Mater.*, 2017, **29**, 1704574.